Scientific Reports

https://doi.org/10.1038/s41598-025-30278-w

Article in Press

Detection of abnormal cortex in patients with orbital fractures

Received: 8 June 2025

Accepted: 24 November 2025

Published online: 06 December 2025

Cite this article as: Ji L., Chen C., Hu J. *et al.* Detection of abnormal cortex in patients with orbital fractures. *Sci Rep* (2025). https://doi.org/10.1038/s41598-025-30278-w

Li-Jun Ji, Cheng Chen, Jin-Yu Hu, Yan-Mei Zeng, Qian Ling, Jie Zou, Liang-Qi He, Xiao-Yu Wang, Hong Wei, Xu Chen, Yi-Xin Wang & Yi Shao

Detection of Abnormal Cortex in Patients with Orbital Fractures

Li-Jun Ji[1]*, Cheng Chen[2,3]*, Jin-Yu Hu[2,3], Yan-Mei Zeng[2,3], Qian Ling[2,3], Jie Zou[2,3], Liang-Qi He[2,3], Xiao-Yu Wang[2,3], Hong Wei[2,3], Xu Chen[4], Yi-Xin Wang[5], Yi Shao[3#],

[1]Department of Ophthalmology, Dahua Hospital, Shanghai200237, China;

[2]Department of Ophthalmology, The First Affiliated Hospital of Nanchang University, Nanchang, Jiangxi 330006, China;

[3]Department of Ophthalmology, Shanghai General Hospital, Shanghai Jiao Tong University School of Medicine, National Clinical Research Center for Eye Diseases, Shanghai 200080, China

[4]Ophthalmology Centre of Maastricht University, Maastricht 6200MS, Limburg AProvincie, Netherlands;

[5]School of optometry and vision science, Cardiff University, Cardiff, CF24 4HQ, Wales;

Correspondence to: Professor: Yi Shao (E-mail: freebee99@163.com), Department of Ophthalmology, Shanghai General Hospital, Shanghai Jiao Tong University School of Medicine, National Clinical Research Center for Eye Diseases, Shanghai 200080, China

*Equal contribution

Abstract

Background: To pinpoint brain areas exhibiting deviations in white and gray matter (GM, WM) among individuals with orbital fractures (OF) through voxel-based morphometry (VBM). Neuroimaging methods are employed to uncover any cortical abnormalities in patients suffering from orbital fractures. The aim is to explore the possible impacts and clinical significance of orbital fractures on brain structure.

Methods: Twenty patients (12 males, 8 females) with OF and 20 (12 males, 8 females) age-, sex-, and education-matched healthy controls (HCs) were enrolled. All subjects underwent magnetic resonance imaging (MRI). Imaging data were analyzed using two sample t tests to identify the between-groups differences in gray and white matter. We used the differences of the WM volume and GM volume values between the two groups as diagnostic markers. The mean values of the WM and GM volumes in different brain regions were extracted and used to analyze Receiver operating characteristic (ROC) curves.

Results: Lower GM density ($P < 0.05$) was found in patients with OF than in healthy subjects in three clusters, the right superior temporal gyrus, the right middle temporal gyrus, the right and left inferior frontal orbital gyrus, the left superior temporal gyrus, the anterior cingulate and the paracingulate gyrus, and the right Insula. In addition, the WM density in patients with OF decreased significantly in the brain regions of the right parahippocampal gyrus and the left superior temporal gyrus ($P < 0.05$). **Conclusion:**

This study found abnormal brain structure in patients with OF based on VBM. We found GM reduction in patients with OF in three clusters and WM reduction in the right parahippocampal gyrus and the left superior temporal gyrus, which may reflect pathologic mechanisms of OF in vision, motor and cognition. Furthermore, ROC curve analysis demonstrated that the mean values of the WM and GM volumes in different brain regions, are expected to be used as an imaging marker for evaluating the effects of orbital frontal trauma on the central nervous system (CNS). This paper presented a research orientation for further exploration.

Keywords: Orbital Fractures; Voxel-based Morphometry; gray matter; white matter; magnetic resonance imaging

Introduction

Orbital fractures are usually caused by blunt trauma to the orbit, involve facial damage and most commonly affect the orbital floor (48.0%) followed by medial wall (25.2%)(1). Statistically, left orbital fractures are more common than those of the right orbit. Orbital fractures are more prevalent in young patients with a mean patient age of 39.3 years and the most common cause of all orbital fractures is assault followed by falls (1-5). The most common type of orbital fracture is orbital blowout which is a traumatic deformity of the orbital floor or medial wall, resulting from impact of a blunt object larger than the orbital aperture, or eye socket. The orbital floor is most prone to collapse, because the bones of the roof and

lateral walls are more robust. And while the medial wall bone is thinnest, it is buttressed by the bone separating the ethmoidal air cells. The comparatively thin bone of the floor of the orbit and roof of the maxillary sinus has no support so the inferior wall is more likely to collapse. Medial wall blowout fractures are less common, while roof and lateral wall blowout fractures are uncommon and rare respectively.

There are two broad categories of blowout fractures: open door, which are large, displaced and comminuted, and trapdoor, which are linear, hinged, and minimally displaced. Both are characterized by diplopia, enophthalmos, eye movement restriction and loss of sensation of the cheek and upper gums due to infraorbital nerve injury (6). In some cases, blowout fractures and comminuted fractures of the orbit may cause the eyeball to collapse, deform the eyeball, especially damage the optic nerve, compress the optic nerve, and cause a sharp decline in vision, which may need surgery. Early detection of optic nerve canal injury, so as to perform optic nerve canal decompression, blocking the secondary injury is very important. Although the sensory and visual pathway disturbances described above can be explained by local trauma, the brain undergoes anterograde degeneration along the visual pathway after optic nerve injury.

The brain's functional regions exhibit asymmetric responses in processing visual information. To identify object boundaries and generate stereoscopic vision, the brain must process light variations. The upper visual field shows relatively stable brightness changes, while the lower visual field experiences more dynamic light variations. This biological contrast likely led to the evolution of enhanced light pathways specifically designed to process visual information from the lower field (7). Optic nerve truncation was performed in a rat model and neuronal cells were found to atrophy, decrease, and apoptosis in the dorsolateral geniculate nucleus (dLGN) and primary visual cortex (V1) (8). Functional imaging of the optic nerve before and after extrusion showed that the ocular dominance of the contralateral primary visual cortex (V1) immediately shifted to the ipsilateral healthy eye after extrusion (9). Subsequently, spontaneous brain activity in the V1 region corresponding to the optic nerve pinched eye decreased. In addition, craniofacial fractures are often complicated by traumatic brain injury. A study of OF repair versus traumatic brain injury showed that about half of patients with OF present with impaired consciousness (10). In conclusion, nerve damage caused by OF can have an impact on the cerebral cortex and alter the function of the cerebral cortex in the subsequent process. However, there are few

studies on the relationship between OF and the cerebral cortex. There are no studies on the detailed and comprehensive mechanistic changes in cerebral cortex activity in patients with OF.

Accurate diagnosis of OF is difficult when based on clinical characteristics alone. The use of modern imaging techniques such as dynamic magnetic resonance imaging may be very helpful in diagnosis, classification and effective treatment of orbital fractures (11). Voxel-based Morphometry (VBM) was first introduced at the turn of the millennium, and has been very frequently used since then to address a range of neuroscientific questions. The principles of VBM have been described in detail previously (12-13). It is a computational approach to neuroanatomy that measures differences in local concentrations of brain tissue, through a voxel-wise comparison of multiple brain images (14). In traditional morphometry, the whole brain or partial brain volume is measured by drawing regions of interest on brain scan images and calculating the volume enclosed (15). However, this is time consuming and can only provide measures of relatively large areas and small differences in volume may be undetected. The value of VBM is that it allows for comprehensive measurement of differences, not only in specific structures, but throughout the entire brain (16). VBM is particularly suitable for exploratory studies covering the whole

brain, which can capture diffuse or unexpected changes. Surface-based morphological analysis (SBM) is also widely used in the study of brain structures, with FreeSurfer software being a typical representative. It not only excels in analyzing the volume of deep nuclear groups but also in examining changes in the cortex and subcortex. SBM can achieve precise segmentation of cortical thickness and surface area and allows for more accurate combined analyses with functional imaging data (17). SBM is good at targeted and precise anatomical analysis because it requires the regions of interest (ROI) rather than exploring whole brain changes.

However, in modern research, VBM and SBM technologies are not mutually exclusive, but complementary. VBM may be sensitive to various artifacts, including misalignment of brain structures, misclassification of tissue types, differences in folding patterns and in cortical thickness (18). VBM cannot distinguish between cortical thickness and surface area. SBM calculations are complex and time-consuming, and the accuracy of results highly depends on the quality of the original images. When images have artifacts, low contrast, or serious lesions (such as tumors or stroke lesions), the automated process is prone to errors (19). Due to the lack of previous research on brain structures in patients with orbital bone

fractures, it is not possible to determine ROI. The purpose of this study is to preliminarily explore the areas that change throughout the brain, hence VBM was chosen as the tool for this research. VBM can evaluate the differences of all brain voxels without strict dependence on anatomical assumptions, which has a unique advantage in detecting post-traumatic diffuse or accidental changes.

It has been hypothesized that OF can cause spontaneous abnormalities in the brain regions. To test this hypothesis, we used VBM to identify the differences of densities/volumes in white and gray matter between patients with OF and healthy controls (HCs). Receiver operating characteristic (ROC) curve was used to verify the clinical significance of brain region changes--whether these brain region changes could serve as an evaluation criterion to assess the presence and severity of neurological damage in OF patients. Neural anomalies of this kind may reflect part of the underlying pathological mechanism of related to OF.

Materials and Methods

Subjects

This research recruited 20 healthy controls (HCs) (12 males, 8 females), who were age-, sex-, and education status-matched to the

patients with OF (12 males, 8 females) from the First Affiliated Hospital of Nanchang University. Patients and HCs with the following conditions were included: 1) Patients with clinical and radiographic diagnosis of orbital fractures and received an MRI scan 2-4 weeks after injury; 2) no nervous system or mental health diseases; 3) no headaches; 4) no history of congenital or acquired diseases such as hypertension, diabetes mellitus, or coronary artery disease, and no addictions such as heroin, smoking, or alcohol; 5) no contraindications for MRI (such as cardiac pacemaker or other embedded metal device); 6) Patients are over eighteen years old.

The research was approved by the medical ethics of the First Affiliated Hospital of Nanchang University. The research was conducted in accordance with the Declaration of Helsinki. Each participant signed a declaration of informed consent.

Structural MRI parameters

Magnetic resonance imaging (MRI) scans were conducted on each participant using a 3-Tesla MR scanner (Siemens, Germany). High-resolution T1-weighted images were acquired with fast gradient echo sequence (magnetization prepared rapid acquisition gradient echo, MP RAGE). The following protocol parameters were used: Slices=176; section thickness=1.0mm; echo time=2.26 ms;

repetition time=1,900 ms; field of view=215x230 mm. All MRI images were evaluated for gross structural abnormalities. No subjects were excluded.

VBM analysis

The MRIcro software (www.mricro.com) was used to visualize MRI T1 weighted images and check to ensure that the images are of high quality for subsequent processing. Following this, the structural images were processed using a voxel-based morphometric toolbox (VBM8; http://dbm.neuro.unijena.de/vbm8/) on a statistical parameter map (SPM 8; http://www.fil.ion.ucl.ac.uk). All procedures were performed on the MATLAB 7.9.0 software (R2009b; The Mathworks, Inc., Natick, MA, USA). Brain images were segmented into parts including gray matter, white matter and cerebrospinal fluid using the VBM8 toolbox. The data were then standardized to meet the Montreal Neurological Institute space criteria. The VBM analyses followed the Diffeomorphic Anatomical Registration Through Exponentiated Lie algebra approach (20). Finally, the volumes were smoothed using a 8/12-mm full-width-at-half-maximum (FWHM) Gaussian kernel. Normalized, modulated, smoothed images were submitted to group-level analyses.

Statistical Analysis

A two-sample *t*-test was used to compare GM and WM between patients with OF and HCs after controlling for the effects of age and sex. The significance level was set at $p<0.05$, Gaussian random field (GRF) theory corrected, minimum $z>2.3$, voxel level $P < 0.01$, and cluster level $P < 0.05$. A significant voxel was superimposed on the normalization of 3DT1wi (three-dimensional magnetization, fast acquisition gradient echo sequence) to acquire a color map. Based on this, we used the receiver operating characteristic (ROC) curve to quantify the discriminative power of VBM in detecting structural brain changes between OF patients and healthy controls.

Results

General data analysis

No significant differences in weight ($p = 0.902$) or age ($p = 0.871$) were found between the OFs and HCs group. See Table 1 for more details.

Table 1. Demographics information and clinical measurements for OFs and HCs

Condition	OFs	HCs	T-value	P-value
M/F	12/8	12/8	N/A	>0.99
Age (years)	51.21±11.42	50.96±10.82	0.242	0.871

Weight (kg)	68.32±9.24	69.93±9.54	0.165	0.902
Duration (days)	11.61±4.14	N/A	N/A	N/A
Handedness	20R	20R	N/A	>0.99
Best-corrected VA-left eye	0.40±0.20	1.05±0.20	-3.763	0.017* Cohen'd=3.25
Best-corrected VA-right eye	0.45±0.15	1.00±0.15	-3.064	0.011* Cohen'd=3.67

Significant at * P<0.05 and P<0.001, independent t test. P, P-value between OF and HCs. OF- Orbital Fractures; HCs-Healthy controls; N/A-not applicable; VA–visual acuity.

Gray and white matter differences

Lower GM density was found in patients with OF than healthy subjects in three clusters, including the right superior temporal gyrus, the right middle temporal gyrus, the right and left inferior frontal orbital gyrus, the left superior temporal gyrus, the anterior cingulate and the paracingulate gyrus, and the right Insula. See Figure 1, Table 2 and Figure 3a for details. The WM density in patients with OF was significantly lower than controls in the brain regions of the right parahippocampal gyrus and the left superior temporal gyrus ($P < 0.05$). See Figure 2, Figure 3b and Table 3 for details.

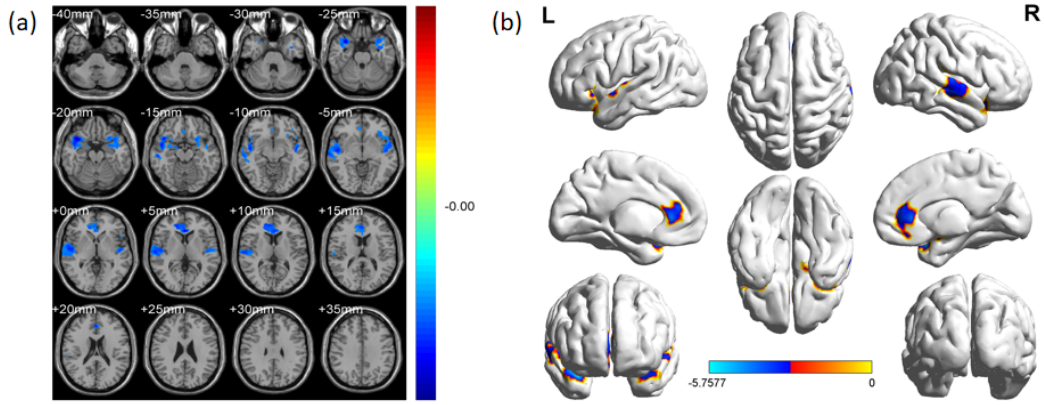

Fig.1 Regional GM decrease in patients with OF compared with HCs. The significantly decreased regions were located in the right superior temporal gyrus, the right middle temporal gyrus, the right and left inferior frontal orbital gyrus, the left superior temporal gyrus, the anterior cingulate and the paracingulate gyrus, and the right Insula. The blue areas denote lower GM brain regions ($P < 0.05$ for multiple comparisons using GRF theory; voxel-wise $P < 0.005$ and cluster-wise $P < 0.05$ corrected). GM, gray matter; OF, orbital fractures; HCs, health controls; L, left; R, right. Use MATLAB 7.9.0 software (R2009b) to generate images, URL: https://www.mathworks.com. Figure 1a was made using RESTplus v1.24, URL: https://github.com/LiXuan1997/RESTplus. Figure 1b was made using BrainNet Viewer 1.7, URL: https://www.nitrc.org/projects/bnv/.

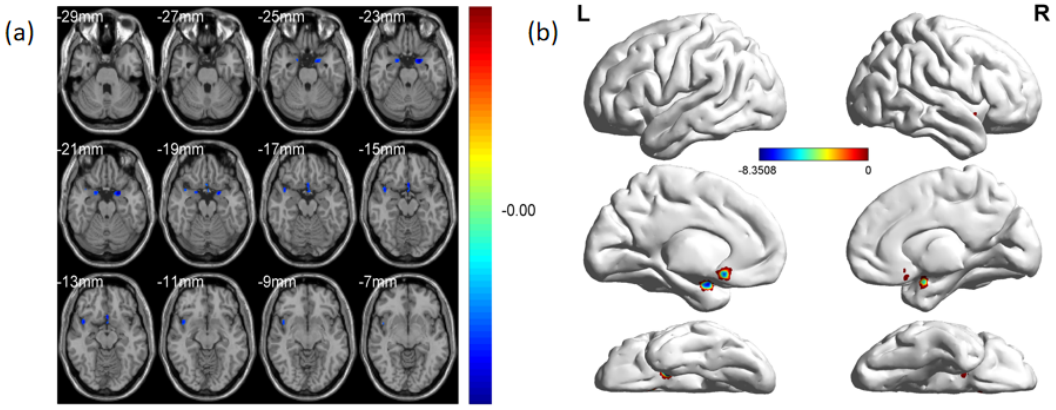

Fig.2 Regional WM decrease in patients with OF compared with HCs. The significantly decreased regions were located in the right parahippocampal gyrus and the left superior temporal gyrus. The blue areas denote lower WM brain regions ($P < 0.05$ for multiple comparisons using GRF theory; voxel-wise $P < 0.005$ and cluster-wise $P < 0.05$ corrected). WM, white matter; OF, orbital

fractures; HCs, health controls; L, left; R, right. Use MATLAB 7.9.0 software (R2009b) to generate images, URL: https://www.mathworks.com. Figure 2a was made using RESTplus v1.24, URL: https://github.com/LiXuan1997/RESTplus. Figure 2b was made using BrainNet Viewer 1.7, URL: https://www.nitrc.org/projects/bnv/.

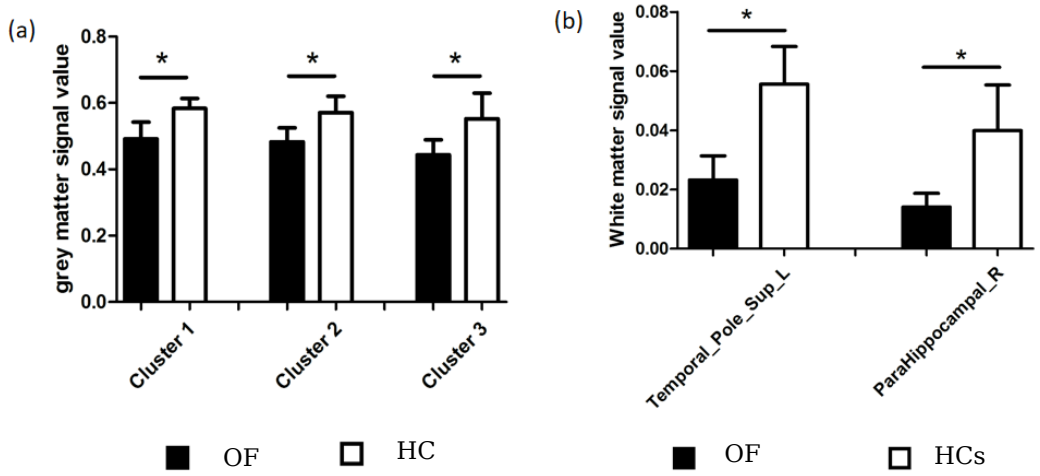

Fig.3 The GM signal values and WM signal values between the OF group and HCs (a, b). GM-grey matter; WM-white matter; OF, Orbital Fractures; HCs, Healthy controls.

Table 2. GM differences between OF and HC groups

Clusters	BA	Brain areas	MNI coordinates			Number of voxels	T value
OFs< HCs			X	Y	Z		
Clusters 1	84	Right temporal pole	36	15	-22.5	1123	-5.7577
		Right superior temporal gyrus				480	
		Right middle temporal gyrus				452	
		Right Insula				301	
		Right inferior frontal orbital gyrus				236	
Clusters 2	81	Left superior temporal gyrus	-46.5	-7.5	-9	939	-4.1181

		Left temporal pole				817	
		Left inferior frontal orbital gyrus				693	
Clusters 3	-	Right anterior cingulate and the paracingulate gyrus	0	30	6	1066	-4.4392
		Left anterior cingulate and the paracingulate gyrus				350	

Abbreviations: BA, Brodmann area; GM, gray matter; MNI, Montreal Neurological Institute; OF, Orbital Fractures; HCs, Healthy controls.

Table 3. WM differences between OF and HC groups

Clusters	**BA**	**Brain areas**	**MNI coordinates**			**Number of voxels**	**T value**
OFs< HCs			**X**	**Y**	**Z**		
	39	Left temporal pole	-19.5	3	-22.5	179	-8.3508
	40	Right parahippocampal gyrus	19.5	3	-22.5	64	-5.936

Abbreviations: BA, Brodmann area; WM, white matter; MNI, Montreal Neurological Institute; OF, Orbital Fractures; HCs, Healthy controls.

Receiver operating characteristic (ROC) curve

ROC curves were used to assess whether structural indicators of the VBM could reliably distinguish OF patients from healthy controls. The mean values of the WM and GM volumes in different brain regions were extracted and used to analyze ROC curves. The areas under the ROC for GM volume values were: 0.939 for cluster

1, 0.918 for cluster 2, and 0.867 for cluster 3 (see Figure 4, Figure 5). The AUCs for WM volume values were: 0.974 for left superior temporal pole and 0.939 for the right parahippocampal gyrus (see Figure 6, Figure 7).

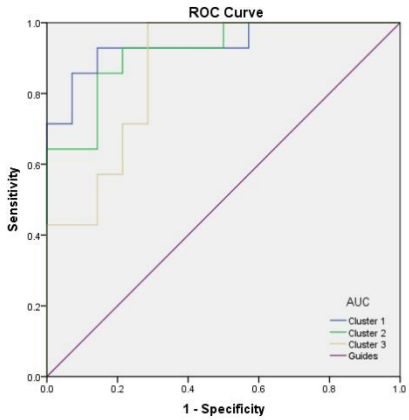

Fig.4 ROC curve analysis of the mean VBM values for altered brain regions in OF patients. The area under the ROC curve were 0.939, (p<0.0001; 95% CI: 0.849-1.000) for Cluster 1; Cluster 2 0.918, (p<0.0001; 95% CI: 0.819-1.000); Cluster 3 0.867, (p=0.001; 95% CI: 0.732-1.000). OF, Orbital Fractures; AUC, area under the curve; ROC, receiver operating characteristic.

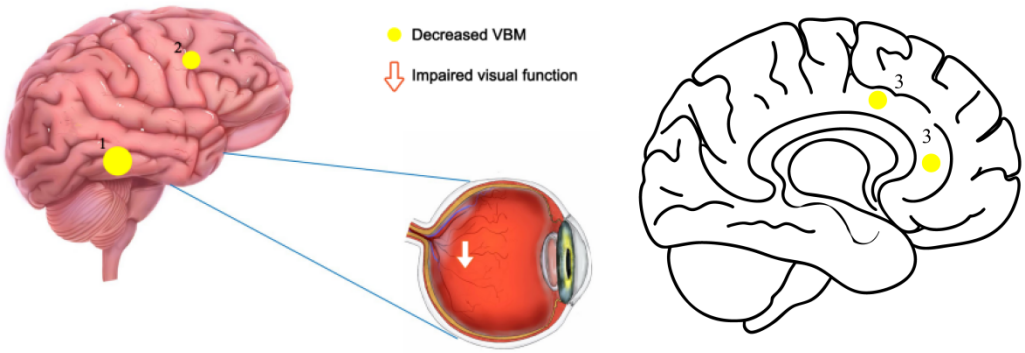

Fig.5 The mean VBM values of altered brain regions in OF patients. Compared with the HCs, the VBM values of the following regions were decreased to various extents: 1- Cluster 1 (BA 84, t = -5.7577), 2- Cluster 2 (BA 81, t = -4.1181), 3- Cluster 3 (t = -4.4392). OF, Orbital Fractures; HCs, healthy controls; BA, Brodmann's area. Made with Adobe Photoshop 2022 (version: v23.0) and Adobe

Illustrator 2025, URL: https://www.adobe.com/products/photoshop.html.

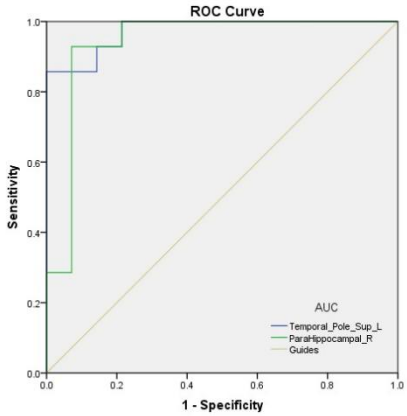

Fig.6 ROC curve analysis of the mean VBM values for altered brain regions in OF patients. The area under the ROC curve were 0.974, (p □ 0.0001; 95% CI: 0.928-1.000) for Temporal_Pole_Sup_L; ParaHippocampal_R 0.939, (p□0.0001; 95% CI: 0.837-1.000). OF, Orbital Fractures; AUC, area under the curve; ROC, receiver operating characteristic.

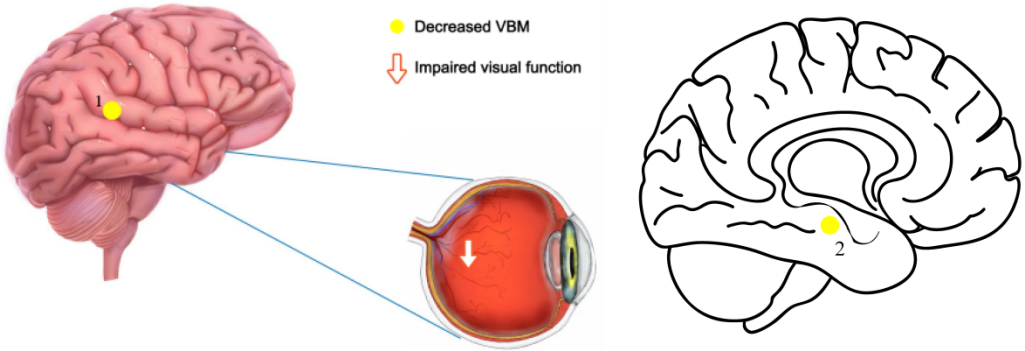

Fig.7 The mean VBM values of altered brain regions in OF patients. Compared with the HCs, the VBM values of the following regions were decreased to various extents: 1- Temporal_Pole_Sup_L (BA 39, t = -8.3508), 2- ParaHippocampal_R (BA 40, t = -5.936). OF, Orbital Fractures; HCs, healthy controls; BA, Brodmann's area. Made with Adobe Photoshop 2022 (version: v23.0) and Adobe Illustrator 2025, URL: https://www.adobe.com/products/photoshop.html.

Discussion

Orbital fractures are common injuries caused by assault or falls (21-23). They may involve pain, swelling, loss of function, or

changes in the shape of facial structures. OF is often accompanied by varying degrees of brain injury, and even mild concussions can cause an inflammatory response in the brain. Traumatic brain injury secondary to OF triggers an inflammatory cascade in the brain, impairing synaptic function, mitochondrial function, neurotransmission, and neuroplasticity, thereby affecting cognition and behavior (24). When trauma occurs, the brain activates glial cells and releases inflammatory factors (such as IL-6, complement) (25-26). Complement promotes persistent neurodegeneration and chronic neuroinflammation, exacerbates brain damage, and causes changes in the function of brain regions (27-28). Traumatic brain injury is closely related to the visual system. In neuroinflammation and complement action caused by brain trauma, complement C3 deposition was found in the retinal genu pectus synapse of the dorsal lateral geniculate nucleus (dLGN), which eventually led to the progression of visual defects (29-30). A study on traumatic brain injury and brain function showed that diffuse traumatic brain injury caused hippocampal dysfunction, and microglia and astrocytes underwent continuous morphological changes during the process of damage (31). Mohamed AZ et al. used diffusion tensor imaging (DTI) to study Diffuse traumatic brain injury and demonstrated that numerous white matter tracts (including the corpus callosum, internal and external capsule, and optic tract) as well as the grey-matter in the cortex, thalamus, and hippocampus in the injured brain were significantly altered in fractional anisotropy (FA) and mean diffusivity (RD) (32).

Optic nerve injury can cause impaired axonal transport in neuronal cells, and IL-6 is a potential marker for the emergence of this phenomenon. In a glaucoma model, IL-6, brain-derived neurotrophic factor (BDNF), and amyloid precursorprotein (APP,

the stereotypical marker of fast axonal transport) have been found to accumulate within axons of the optic nerve head (ONH) (33). Axonal transport deficits are an early key pathologic feature of optic nerve cell death and neurodegeneration (34). Impaired axonal transport not only affects its own neurons, but also causes functional changes in the corresponding brain regions. Kim, K. et al. demonstrated that unilateral optic nerve injury induces asymmetric elevation of glucose metabolism in the visual cortex (primary visual center) region bilaterally (more pronounced elevation in the visual cortex on the side corresponding to the injured eye), as well as bilateral elevation of glucose metabolism in the thalamus region (no asymmetry was detected), with no significant changes in other regions were not significantly altered (35).

OF predisposes to trigeminal nerve damage. Peripheral nerves in the craniofacial and periorbital areas transmit pain stimulus information to the trigeminal ganglion/trigeminal nucleus, which in turn passes through the thalamus to project widely to multiple cortical areas such as the medial frontal pole, the anterior pyriform cortex, the orbital gyrus cortex, the anterior cingulate gyrus, the insula, etc (36-39). Studies have shown that trigeminal pain is associated with reduced grey matter in the thalamus, cingulate gyrus, head of the caudate nucleus, bilateral inguinal, superior, middle, and transverse temporal gyrus, subcallosal gyrus, anterior cingulate cortex, bilateral insulae, vestibular gyrus, postcentral gyrus, bilateral middle frontal gyrus, and anterior cerebellar lobes (40).

In this study, we found that reduced GM volume in the right superior and middle temporal gyri, the right and left inferior frontal orbital gyri, the left superior temporal gyrus, the anterior cingulate and the paracingulate gyrus, and the right Insula area (Figure 1,

Table 2, Figure 3a) in patients with OF compared with healthy subjects. In addition, the WM volume in the right parahippocampal gyrus and the left superior temporal gyrus (Figure 2, Table 3, Figure 3b) were all lower in patients with OF than healthy subjects. ROC results suggested that changes in activity in these regions can be used to distinguish OF from healthy populations and suggest potential neural mechanisms for OF (Figure 4, Figure 5, Figure 6, Figure 7) . By supplementing t-test analysis with quantitative diagnostic accuracy rather than merely reporting statistical significance, this approach facilitates the clinical translation of our VBM research findings. ROC results demonstrate that structural brain changes identified through VBM hold promise as imaging biomarkers for evaluating orbital trauma's impact on the central nervous system (CNS). These findings also enhance the potential to provide early targeted interventions for patients, thereby mitigating long-term CNS effects.

The superior temporal gyrus contains the auditory cortex, which is responsible for processing sounds, and Wernicke's area, which is located in the left hemisphere and is involved in the comprehension of language (41-42). The posterior part of the superior temporal gyrus of the cerebral cortex harbors the H area (auditory speech center), thus auditory aphasia is obtained when the posterior part of the superior temporal gyrus of the cerebral cortex is damaged (43). In addition to auditory and language processing, the superior temporal gyrus has been implicated as an

important structure in social cognition. Medial temporal gyrus structures that are critical for long-term memory include the hippocampus, and the surrounding perirhinal, parahippocampal, and entorhinal neocortical regions (44). The hippocampus is critical for memory formation, and the surrounding medial temporal cortex is currently theorized to be critical for memory storage. Our findings of reduced volume in the parahippocampal region and superior temporal gyrus suggest that OF may affect memory and auditory function.

The human insular cortex is a portion of the cerebral cortex folded deep within each hemisphere of the brain. Four functionally distinct areas exist within the human insular cortex: (1) the sensorimotor area located in the central PI, (2) the central olfactory taste area, (3) the social-emotional area located in the anteroventral insula, and (4) the cognitive anterodorsal area (45). Different functional subdivisions of the insula can also act in concert during an fMRI scan, integrating information within and between cognitive, emotional, visual and sensorimotor networks (46). It is believed to be involved in consciousness and play a role in diverse functions usually linked to emotion or the regulation of homeostasis (47-48). These functions include compassion and empathy, taste, perception, motor control, self-awareness,

cognitive functioning, and interpersonal experience (49-53). They are also related to psychopathology, thus we infer that OF may involve loss of these functions, since gray matter is lost in the right insula.

The inferior frontal gyrus has a number of functions including language comprehension, speech production, semantic processing, fine motor control, endoreceptive awareness and emotion. (54-58). The left opercular part of the inferior frontal gyrus is a part of the articulatory network involved in motor syllable programs (59-60). The inferior frontal orbital gyrus is part of the prefrontal cortex network which has been implicated in executive functions, such as cognition, decision making, and attention. PFC is involved in the process of transforming raw visual inputs are transformed into abstractions (61). One study used non-zero disparity checkerboards to stimulate the PFC of macaque monkey where hyperactivation has been observed (62). Bilateral inferior frontal orbital gyri have a role in completion of goal-directed motion as part of the PFC network (63). Therefore, the reduced GM in the inferior frontal gyrus in the present study may reflect pathology of mechanisms related to disparity processing and visual cognition.

The cingulate gyrus is an important component of the limbic system, mainly involved in the expression of emotions and the

regulation of visceral activity, autonomic function, motor function and the perception of pain (64). The cingulate gyrus receives inputs from the thalamus and the neocortex, and projects to the entorhinal cortex via the cingulum. It plays a role in executive function and respiratory control, and is an integral part of the limbic system, with roles in emotion formation and processing, learning, and memory (65-66). The latter three functions together make the cingulate gyrus highly influential in linking motivational outcomes to behavior, and important in such as depression and schizophrenia (66). Reduced GM in the present study may manifest as inhibition of the above functions.

Limitations

This study has yielded promising positive results and presents a novel perspective that "brain activity in OF patients differs from healthy individuals," while opening up new avenues for understanding the pathogenesis of OF. However, we must acknowledge six limitations: (1) Although statistically robust, the small sample size limits the findings' generalizability. (2) The research only preliminarily explored changes in brain activity without subgroup analysis based on fracture type or side, and its cross-sectional nature precludes causal inference. (3) Potential confounding factors such as psychological stress or systemic

trauma were not addressed. (4) Other clinical variables that might influence the results—such as post-injury duration, presence of secondary traumatic brain injury, and severity—were not accounted for. (5) More peripheral injury evaluation indicators, such as eye movement function, exophthalmos and orbital imaging changes, were not included in the study. (6) This study did not combine SBM technology to conduct a more comprehensive study of the topic.

Conclusions

To conclude, in this VBM study of patients with OF we found that, one month after the injury, GM reductions in gray and white matter found in specific brain regions of patients with OF provide evidence of neural changes following this injury, and indicate pathological changes in this condition. These changes may trigger the pathogenesis of loss of sensation, body disfunction and adversely affect the function of the visual cortex in patients with OF. In the future, we will add some paradigms to evaluate the function of the visual cortex and combine MRI to explore their connection in patients with OF.

Declarations

Author Contributions

Li-Jun Ji and Cheng Chen participated in Writing – Original Draft,

Review & Editing, Formal Analysis, figure 7 and Methodology; Jie Zou, Jin-Yu Hu, Qian Ling and Yan-Mei Zeng participated in table 1-3, figure 1-3 and Writing – Review & Editing and Data Curation; Xiao-Yu Wang, Liang-Qi He and Hong Wei participated in figure 4-6 and Writing – Review & Editing; Xu Chen and Yi-Xin Wang participated in Conceptualization, Validation and Project Administration; Yi Shao participated in Resources, Software and Validation.

Funding

Not applicable.

Ethical considerations

The Medical Ethics Committee of the First Affiliated Hospital of Nanchang University approved the study's methodology (cdyfy 2021039), and the study adhered to the Declaration of Helsinki.

Patient consent for participation and publication

All participants received information about the objectives, strategies, steps, and inherent hazards involved in the study before providing written informed consent to participate. Written informed consent has been obtained from the patient(s) to publish this paper.

Availability of data and materials

The datasets used and/or analyzed during the present study are available from the corresponding author on reasonable request.

Acknowledgments

Not applicable.

Competing interests

This study did not receive any industrial support. The authors have no competing interests to declare regarding this study.

References

[1].Chiang, E., Saadat, L. V., Spitz, J. A., Bryar, P. J., & Chambers, C. B. (2016). Etiology of orbital fractures at a level I trauma center in a large metropolitan city. Taiwan journal of ophthalmology, 6(1), 26–31. https://doi.org/10.1016/j.tjo.2015.12.002.

[2].Caranci, F; Cicala, D; Cappabianca, S; Briganti, F; Brunese, L; Fonio, P (2012). "Orbital fractures: Role of imaging". Seminars in Ultrasound, CT and MRI. 33 (5): 385–91. doi:10.1053/j.sult.2012.06.007. PMID 22964404.

[3].Lin, K. Y., Ngai, P., Echegoyen, J. C., & Tao, J. P. (2012). Imaging in orbital trauma. Saudi journal of ophthalmology: official journal of the Saudi Ophthalmological Society, 26(4), 427–432. https://doi.org/10.1016/j.sjopt.2012.08.002

[4].Kunz, C., Audigé, L., Cornelius, C. P., Buitrago-Téllez, C. H., Rudderman, R., & Prein, J. (2014). The Comprehensive AOCMF Classification System: Orbital Fractures - Level 3 Tutorial. Craniomaxillofacial trauma & reconstruction, 7 (Suppl 1), S092–S102. https://doi.org/10.1055/s-0034-1389562

[5].Snäll, J., Narjus-Sterba, M., Toivari, M., Wilkman, T., & Thorén, H. (2019). Does postoperative orbital volume predict postoperative globe malposition after blow-out fracture reconstruction? A 6-month clinical follow-up study. Oral and maxillofacial surgery, 23(1), 27–34. https://doi.org/10.1007/s10006-019-00748-3

[6].Runci, M., De Ponte, F. S., Falzea, R., Bramanti, E., Lauritano, F., Cervino, G., Famà, F., Calvo, A., Crimi, S., Rapisarda, S., & Cicciù, M. (2017). Facial and Orbital Fractures: A Fifteen Years Retrospective Evaluation of North East Sicily Treated Patients. The open dentistry journal, 11, 546–556. https://doi.org/10.2174/1874210601711010546

[7]. Scott MTW, Yakovleva A, Norcia AM. Visual Field Asymmetries in Responses to ON and OFF Pathway Biasing Stimuli. Vis Neurosci. 2024 Dec 19;41:E007. doi: 10.1017/S095252382400004X. PMID: 39698978; PMCID: PMC11730990.

[8]. You Y, Gupta VK, Graham SL, Klistorner A. Anterograde degeneration along the visual pathway after optic nerve injury. PLoS One. 2012;7(12):e52061.

[9].Vasalauskaite A, Morgan JE, Sengpiel F. Plasticity in Adult

Mouse Visual Cortex Following Optic Nerve Injury. Cereb Cortex. 2019;29(4):1767-1777. doi:10.1093/cercor/bhy347
[10].Malla A, Hassan B, Er S, et al. Traumatic Brain Injury and Its Association With Orbital Fracture Characteristics and Repair. J Craniofac Surg. Published online June 28, 2024.
[11].Loba, P., Kozakiewicz, M., Elgalal, M., Stefa ń czyk, L., Broniarczyk-Loba, A., & Omulecki, W. (2011). The use of modern imaging techniques in the diagnosis and treatment planning of patients with orbital floor fractures. Medical science monitor: international medical journal of experimental and clinical research, 17(8), CS94–CS98. https://doi.org/10.12659/msm.881889
[12]. Ashburner, John; Friston, Karl J. (June 2000). "Voxel-Based Morphometry—The Methods". NeuroImage. 11 (6): 805–21. CiteSeerX 10.1.1.114.9512. doi:10.1006/nimg.2000.0582. PMID 10860804.
[13]. Gale SD, Baxter L, Roundy N, et al. Traumatic brain injury and grey matter concentration: a preliminary voxel based morphometry study. Journal of Neurology, Neurosurgery & Psychiatry 2005;76:984-988.
[14]. Anderson M. Winkler; Peter Kochunov; John Blangero; Laura Almasy; Karl Zilles; Peter T. Fox; Ravindranath Duggirala; David C. Glahn (2010). "Cortical thickness or grey matter volume? The importance of selecting the phenotype for imaging genetics studies". NeuroImage. 53 (3): 1135–46. doi:10.1016/j.neuroimage.2009.12.028. PMC 2891595. PMID 20006715.
[15].Yasuhiro Kawasaki, Michio Suzuki, Ferath Kherif, Tsutomu Takahashi, Shi-Yu Zhou, Kazue Nakamura, Mie Matsui, Tomiki Sumiyoshi, Hikaru Seto and Masayoshi Kurachi (January 2007). "Multivariate voxel-based morphometry successfully differentiates schizophrenia patients from healthy controls". NeuroImage. 34 (1): 235–242. doi:10.1016/j.neuroimage.2006.08.018. PMID 17045492.
[16].Natalie L. Voets; Morgan G. Hough; Gwenaëlle Douaud; Paul M. Matthews; Anthony James; Louise Winmill; Paula Webster; Stephen Smith (2008). "Evidence for abnormalities of cortical development in adolescent-onset schizophrenia". NeuroImage. 43 (4): 665–75.
[17]. Goto M, Abe O, Hagiwara A, Fujita S, Kamagata K, Hori M, Aoki S, Osada T, Konishi S, Masutani Y, Sakamoto H, Sakano Y, Kyogoku S, Daida H. Advantages of Using Both Voxel- and Surface-based Morphometry in Cortical Morphology Analysis: A Review of Various Applications. Magn Reson Med Sci. 2022 Mar 1;21(1):41-57. doi: 10.2463/mrms.rev.2021-0096. Epub 2022 Feb 18. PMID: 35185061; PMCID: PMC9199978.
[18].Yang, C., Chang, J., Liang, X., Bao, X., & Wang, R. (2020). Gray

Matter Alterations in Parkinson's Disease With Rapid Eye Movement Sleep Behavior Disorder: A Meta-Analysis of Voxel-Based Morphometry Studies. Frontiers in aging neuroscience, 12, 213. https://doi.org/10.3389/fnagi.2020.00213.

[19]. Righart R, Schmidt P, Dahnke R, Biberacher V, Beer A, Buck D, Hemmer B, Kirschke JS, Zimmer C, Gaser C, Mühlau M. Volume versus surface-based cortical thickness measurements: A comparative study with healthy controls and multiple sclerosis patients. PLoS One. 2017 Jul 6;12(7):e0179590. doi: 10.1371/journal.pone.0179590. PMID: 28683072; PMCID: PMC5500013.

[20].J. Ashburner, Re: Differences Between DARTEL and SHOOT Templates, Message to the SPM list, Available at https://www.jiscmail.ac.uk/cgi-bin/webadmin?A2=SPM;486a38f9.1705 (last accessed 11 May 2017), 2017.

[21]. Lozada, K. N., Cleveland, P. W., & Smith, J. E. (2019). Orbital Trauma. Seminars in plastic surgery, 33(2), 106–113. https://doi.org/10.1055/s-0039-1685477

[22].Oppenheimer, A. J., Monson, L. A., & Buchman, S. R. (2013). Pediatric orbital fractures. Craniomaxillofacial trauma & reconstruction, 6(1), 9–20. https://doi.org/10.1055/s-0032-1332213

[23].Ang, C. H., Low, J. R., Shen, J. Y., Cai, E. Z., Hing, E. C., Chan, Y. H., Sundar, G., & Lim, T. C. (2015). A Protocol to Reduce Interobserver Variability in the Computed Tomography Measurement of Orbital Floor Fractures. Craniomaxillofacial trauma & reconstruction, 8(4), 289–298. https://doi.org/10.1055/s-0034-1399800

[24].Orr TJ, Lesha E, Kramer AH, et al. Traumatic Brain Injury: A Comprehensive Review of Biomechanics and Molecular Pathophysiology. World Neurosurg. 2024;185:74-88. doi:10.1016/j.wneu.2024.01.084

[25].Jamjoom AAB, Rhodes J, Andrews PJD, Grant SGN. The synapse in traumatic brain injury. Brain. 2021;144(1):18-31. doi:10.1093/brain/awaa321

[26].Mira RG, Lira M, Cerpa W. Traumatic Brain Injury: Mechanisms of Glial Response. Front Physiol. 2021;12:740939. Published 2021 Oct 22. doi:10.3389/fphys.2021.740939

[27].Alawieh A, Langley EF, Weber S, Adkins D, Tomlinson S. Identifying the Role of Complement in Triggering Neuroinflammation after Traumatic Brain Injury. J Neurosci. 2018;38(10):2519-2532. doi:10.1523/JNEUROSCI.2197-17.2018

[28].Ciechanowska A, Ciapała K, Pawlik K, et al. Initiators of Classical and Lectin Complement Pathways Are Differently Engaged after Traumatic Brain Injury-Time-Dependent Changes in the Cortex, Striatum, Thalamus and Hippocampus in a Mouse

Model. Int J Mol Sci. 2020;22(1):45. Published 2020 Dec 22. doi:10.3390/ijms22010045
[29].Borucki DM, Rohrer B, Tomlinson S. Complement propagates visual system pathology following traumatic brain injury. J Neuroinflammation. 2024;21(1):98. Published 2024 Apr 17. doi:10.1186/s12974-024-03098-4
[30].Borucki DM, Toutonji A, Couch C, Mallah K, Rohrer B, Tomlinson S. Complement-Mediated Microglial Phagocytosis and Pathological Changes in the Development and Degeneration of the Visual System. Front Immunol. 2020;11:566892. Published 2020 Sep 24. doi:10.3389/fimmu.2020.566892
[31].Arora P, Trivedi R, Kumari M, et al. Altered DTI scalars in the hippocampus are associated with morphological and structural changes after traumatic brain injury. Brain Struct Funct. 2024;229(4):853-863. doi:10.1007/s00429-024-02758-8
[32].Mohamed AZ, Corrigan F, Collins-Praino LE, Plummer SL, Soni N, Nasrallah FA. Evaluating spatiotemporal microstructural alterations following diffuse traumatic brain injury. Neuroimage Clin. 2020;25:102136. doi:10.1016/j.nicl.2019.102136
[33].G. Chidlow, A. Ebneter, M. C. Holman, J. P. Wood, R. Casson; Axonal Transport Disruption at the Optic Nerve Head: Comparison Between Rat Models of Retinal Ganglion Cell Degeneration and Utility of the Novel Marker Interleukin-6. Invest. Ophthalmol. Vis. Sci. 2010;51(13):2103.
[34].Guo W, Stoklund Dittlau K, Van Den Bosch L. Axonal transport defects and neurodegeneration: Molecular mechanisms and therapeutic implications. Semin Cell Dev Biol. 2020;99:133-150. doi:10.1016/j.semcdb.2019.07.010
[35].Kim, K., Choi, H. young, Pak, K., & Jeon, H. (2020). Changes in brain glucose metabolism following traumatic optic neuropathy in rats. All Life, 14(1), 57–65. https://doi.org/10.1080/26895293.2020.1861110
[36].Price S, Daly DT. Neuroanatomy, Trigeminal Nucleus. In: StatPearls. Treasure Island (FL): StatPearls Publishing; May 1, 2023.
[37].Terrier LM, Hadjikhani N, Destrieux C. The trigeminal pathways. J Neurol. 2022;269(7):3443-3460. doi:10.1007/s00415-022-11002-4
[38].Vertes RP, Hoover WB, Do Valle AC, Sherman A, Rodriguez JJ. Efferent projections of reuniens and rhomboid nuclei of the thalamus in the rat. J Comp Neurol. 2006;499(5):768-796. doi:10.1002/cne.21135
[39].Apkarian AV, Bushnell MC, Treede RD, Zubieta JK. Human brain mechanisms of pain perception and regulation in health and

disease. Eur J Pain. 2005;9(4):463-484. doi:10.1016/j.ejpain.2004.11.001
[40].Henssen D, Dijk J, Knepflé R, Sieffers M, Winter A, Vissers K. Alterations in grey matter density and functional connectivity in trigeminal neuropathic pain and trigeminal neuralgia: A systematic review and meta-analysis. Neuroimage Clin. 2019;24:102039. doi:10.1016/j.nicl.2019.102039
[41].Erin D. Bigler, Sherstin Mortensen, E. Shannon Neeley, Sally Ozonoff, Lori Krasny, Michael Johnson, Jeffrey Lu, Sherri L. Provencal, William McMahon & Janet E. Lainhart (2007): Superior Temporal Gyrus, Language Function, and Autism, Developmental Neuropsychology, 31:2, 217-238
[42].Radua, Joaquim; Phillips, Mary L.; Russell, Tamara; Lawrence, Natalia; Marshall, Nicolette; Kalidindi, Sridevi; El-Hage, Wissam; McDonald, Colm; Giampietro, Vincent; Brammer, Michael J.; David, Anthony S.; Surguladze, Simon A. (2010). "Neural response to specific components of fearful faces in healthy and schizophrenic adults". NeuroImage. 49 (1): 939–946. doi:10.1016/j.neuroimage.2009.08.030. PMID 19699306.
[43]. Le H, Lui MY. Aphasia. 2022 Apr 30. In: StatPearls [Internet]. Treasure Island (FL): StatPearls Publishing; 2022 Jan–. PMID: 32644741.
[44].Kasai K, Shenton ME, Salisbury DF, Hirayasu Y, Lee C-U, Ciszewski AA, et al. Progressive decrease of left superior temporal gyrus gray matter volume in patients with first-episode schizophrenia. Am J Psychiatry 2003a;160:156–64.
[45]. Uddin LQ, Nomi JS, Hébert-Seropian B, Ghaziri J, Boucher O. Structure and Function of the Human Insula. J Clin Neurophysiol. 2017 Jul;34(4):300-306. doi:10.1097/WNP.0000000000000377. PMID: 28644199; PMCID: PMC6032992.
[46]. Gogolla N. The insular cortex. Curr Biol. 2017 Jun 19;27(12):R580-R586. doi: 10.1016/j.cub.2017.05.010. PMID: 28633023.
[47].Phan KL, Wager T, Taylor SF, Liberzon I (June 2002). "Functional neuroanatomy of emotion: a meta-analysis of emotion activation studies in PET and fMRI". NeuroImage. 16 (2): 331–48. doi:10.1006/nimg.2002.1087. PMID 12030820. S2CID 7150871.
[48].Quarto, Tiziana; Blasi, Giuseppe; Maddalena, Chiara; Viscanti, Giovanna; Lanciano, Tiziana; Soleti, Emanuela; Mangiulli, Ivan; Taurisano, Paolo; Fazio, Leonardo (2016-02-09). "Association between Ability Emotional Intelligence and Left Insula during Social Judgment of Facial Emotions". PLOS ONE. 11 (2): e0148621.
[49].Wager, Tor (June 2002). "Functional Neuroanatomy of Emotion: A Meta-Analysis of Emotion Activation Studies in PET and fMRI".

NeuroImage. 16 (2): 331–48. doi:10.1006/nimg.2002.1087. PMID 12030820. S2CID 7150871.
[50].Craig, A. D. (Bud) (2009). "How do you feel — now? The anterior insula and human awareness" (PDF). Nature Reviews Neuroscience. 10 (1): 59–70. doi:10.1038/nrn2555. PMID 19096369. S2CID 2340032. Archived from the original (PDF) on 2013-01-07.
[51].Chen, Z., Chen, X., Liu, M., Ma, L., & Yu, S. (2019). Volume of Hypothalamus as a Diagnostic Biomarker of Chronic Migraine. Frontiers in neurology, 10, 606. https://doi.org/10.3389/fneur.2019.00606
[52].Lan, D. Y., Zhu, P. W., He, Y., Xu, Q. H., Su, T., Li, B., Shi, W. Q., Lin, Q., Yang, Y. C., Yuan, Q., Fang, J. W., Li, Q. H., & Shao, Y. (2019). Gray Matter Volume Changes in Patients With Acute Eye Pain: A Voxel-Based Morphometry Study. Translational vision science & technology, 8(1), 1. https://doi.org/10.1167/tvst.8.1.1
[53].Chechlacz, M., Terry, A., Demeyere, N., Douis, H., Bickerton, W. L., Rotshtein, P., & Humphreys, G. W. (2013). Common and distinct neural mechanisms of visual and tactile extinction: A large scale VBM study in sub-acute stroke. NeuroImage. Clinical, 2, 291–302. https://doi.org/10.1016/j.nicl.2013.01.013.
[54].Sharot, T., Kanai, R., Marston, D., Korn, C. W., Rees, G. & Dolan, R.J. (2012) Selectively Altering Belief Formation in the Human Brain. Proceedings of the National Academy of Sciences, 109 (42), 17058–17062.
[55].Fauci, et.al, eds. (1998), The "dominant inferior frontal convolution" — Harrison's Principles of Internal Medicine, 14th Edition, Companion Handbook, ISBN 978-0-07-021530-6. p.1055
[56].Knoch D, Gianotti LR, Pascual-Leone A, Treyer V, Regard M, Hohmann M, Brugger P (2006). "Disruption of right prefrontal cortex by low-frequency repetitive transcranial magnetic stimulation induces risk-taking behavior" (PDF). J Neurosci. 26 (24): 6469–6472. doi:10.1523/JNEUROSCI.0804-06.2006. PMID 16775134.
[57].Christopoulos, GI.; Tobler, PN.; Bossaerts, P.; Dolan, RJ.; Schultz, W. (Oct 2009). "Neural correlates of value, risk, and risk aversion contributing to decision making under risk". J Neurosci. 29 (40): 12574–83. doi:10.1523/JNEUROSCI.2614-09.2009. PMC 2794196. PMID 19812332.
[58].Fecteau S, Pascual-Leone A, Zald DH, Liguori P, Théoret H, Boggio PS, Fregni F (2007). "Activation of prefrontal cortex by transcranial direct current stimulation reduces appetite for risk during ambiguous decision making". J Neurosci. 27 (23): 6212–6218. doi:10.1523/JNEUROSCI.0314-07.2007. PMID 17553993.
[59].Christopoulos, GI.; Tobler, PN.; Bossaerts, P.; Dolan, RJ.;

Schultz, W. (Oct 2009). "Neural correlates of value, risk, and risk aversion contributing to decision making under risk". J Neurosci. 29 (40): 12574–83. doi:10.1523/JNEUROSCI.2614-09.2009. PMC 2794196. PMID 19812332.
[60].Krauzlis, R. J., Goffart, L., & Hafed, Z. M. (2017). Neuronal control of fixation and fixational eye movements. Philosophical transactions of the Royal Society of London. Series B, Biological sciences, 372(1718), 20160205. https://doi.org/10.1098/rstb.2016.0205)
[61].Xu X, Han Q, Lin J, Wang L, Wu F, Shang H. Grey matter abnormalities in Parkinson's disease: a voxel-wise meta-analysis. Eur J Neurol. 2020 Apr;27(4):653-659. doi: 10.1111/ene.14132. Epub 2019 Dec 23. PMID: 31770481.
[62].Haile, T. M., Bohon, K. S., Romero, M. C., & Conway, B. R. (2019). Visual stimulus-driven functional organization of macaque prefrontal cortex. NeuroImage, 188, 427–444. https://doi.org/10.1073/pnas.1717075115
[63].Suzuki F, Sato N, Ota M, Sugiyama A, Shigemoto Y, Morimoto E, Kimura Y, Wakasugi N, Takahashi Y, Futamura A, Kawamura M, Ono K, Nakamura M, Sano A, Watanabe M, Matsuda H, Abe O. Discriminating chorea-acanthocytosis from Huntington's disease with single-case voxel-based morphometry analysis. J Neurol Sci. 2020 Jan 15;408:116545. doi: 10.1016/j.jns.2019.116545. Epub 2019 Oct 21. PMID: 31704285.
[64]. Vogt BA. Cingulate cortex in the three limbic subsystems. Handb Clin Neurol. 2019;166:39-51. doi: 10.1016/B978-0-444-64196-0.00003-0. PMID: 31731924.
[65].Brincat, S. L., Siegel, M., von Nicolai, C., & Miller, E. K. (2018). Gradual progression from sensory to task-related processing in cerebral cortex. Proceedings of the National Academy of Sciences of the United States of America, 115(30), E7202–E7211.
[66].Haile, T. M., Bohon, K. S., Romero, M. C., & Conway, B. R. (2019). Visual stimulus-driven functional organization of macaque prefrontal cortex. NeuroImage, 188, 427–444. https://doi.org/10.1016/j.neuroimage.2018.11.060